Journal of Hydrology: Regional Studies 12 (2017) 165–180

Contents lists available at ScienceDirect

Journal of Hydrology: Regional Studies

journal homepage: www.elsevier.com/locate/ejrh

Groundwater age determination using ^{85}Kr and multiple age tracers (SF_6, CFCs, and ^{3}H) to elucidate regional groundwater flow systems

Makoto Kagabu[a,*], Midori Matsunaga[b], Kiyoshi Ide[b], Noriyuki Momoshima[c], Jun Shimada[b]

[a] Graduate School of Fisheries and Environmental Sciences, Nagasaki University, 1-14 Bunkyo-machi, Nagasaki 852-8521, Japan
[b] Graduate School of Science and Technology, Kumamoto University, 2-39-1, Kumamoto, Kurokami, 860-8555, Japan
[c] Radioisotope Center, Kyushu University, 6-10-1 Hakozaki, Higashi-ku, Fukuoka 812-8581, Japan

ARTICLE INFO

Keywords:
Krypton-85
Young groundwater dating
Multiple age tracers
Groundwater management
Kumamoto area

ABSTRACT

Study region: The Kumamoto area (945 km^2) in the south of Japan, where almost 100% of the drinking water is dependent on groundwater.
Study focus: Simultaneous measurement of groundwater dating tracers (^{85}Kr, chlorofluorocarbons [CFCs], sulphur hexafluoride [SF_6], and ^{3}H) was performed in the Kumamoto area, to elucidate the regional groundwater flow system and obtain improved estimates of groundwater ages. The groundwater ages were estimated from the ^{85}Kr concentrations in nine locations from three areas: along two major groundwater flow lines (A–A' and B–B'); and a high-nitrate-input recharge area (C area).
New hydrological insights for the region: The groundwater ages could not be estimated using CFCs or SF_6, particularly in the urban areas because of artificial additions to the concentration over almost the entire study area. However, even in these regional circumstances, apparent ages of approximately 16, 36, and not less than 55 years were obtained for three locations on the A–A' line (recharge area, discharge area, and stagnant zone of groundwater, respectively) from ^{85}Kr measurements. This trend was also supported by lumped parameter model analysis using a time series of ^{3}H observations. In contrast, along the B–B' line, the groundwater age of not less than 55 years at three locations, including the recharge to discharge area, where CFCs and SF_6 were not detected, implies old groundwater: this is also the area in which denitrification occurs. In the C area, very young groundwater was obtained from shallow water and older groundwater was detected at greater depths, as supported by the long-term fluctuations of the NO_3^-–N concentration in the groundwater. The results of this study can be effectively used as a "time axis" for sustainable groundwater use and protection of groundwater quality in the study area, where groundwater accounts for almost 100% of the drinking water resources.

1. Introduction

Estimating the age of groundwater is important for the identification of groundwater flow mechanisms as well as for sustainable water utilization. Information on groundwater age also helps to elucidate the evolution of water quality. The majority of groundwater

* Corresponding author.
E-mail address: kagabu@nagasaki-u.ac.jp (M. Kagabu).

http://dx.doi.org/10.1016/j.ejrh.2017.05.003
Received 27 September 2016; Received in revised form 10 May 2017; Accepted 11 May 2017

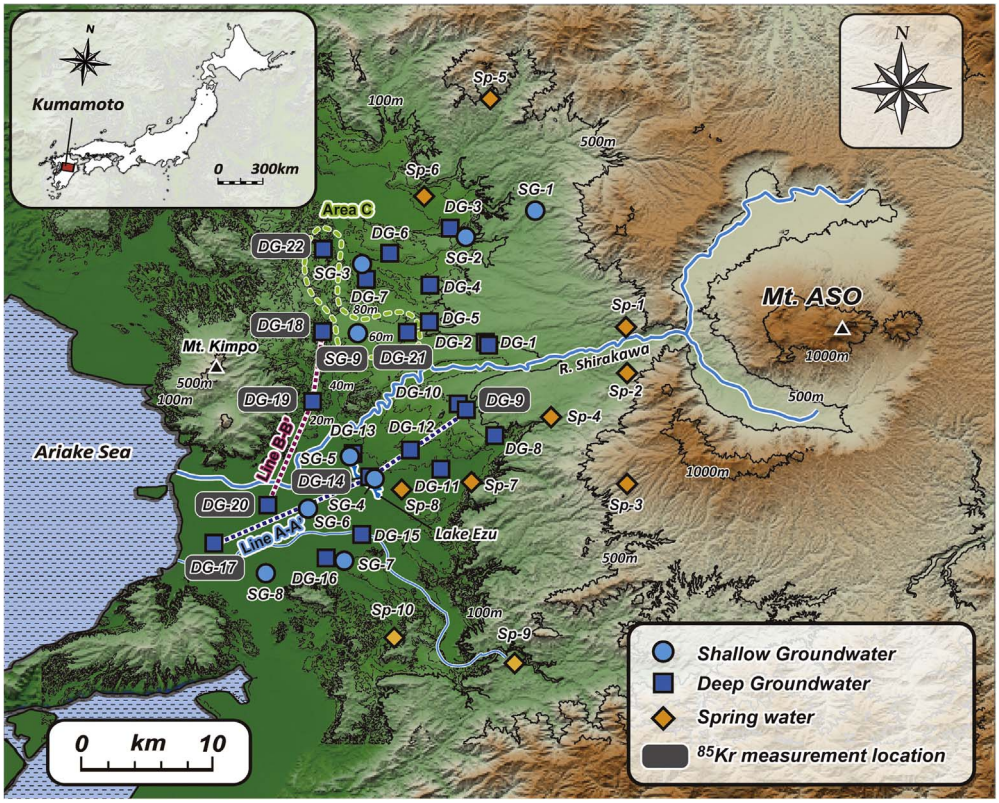

Fig. 1. Location map showing the Kumamoto area including the sampling points.

is presumed to be *young* because active groundwater flow systems exist in Japan as a result of the hydrological environment created by the steep topography and abundant precipitation. In fact, several studies have demonstrated the existence of such *young* groundwater (Asai and Tsujimura, 2009; Asai et al., 2011; Kagabu et al., 2011; Kazahaya et al., 2007). In the Kumamoto area of southern Japan, the subject area of this study, young groundwater is expected to be dominant because of the hydrogeologically good permeability attributable to the porous pyroclastic flow aquifer and steep hydraulic gradient. Globally, many studies have examined young groundwater using hydrogeochemical dating tracers. In recent years, some studies have used tracers of multiple parameters simultaneously in the same area to obtain more accurate dating (Gal et al., 2012; Gooddy et al., 2006; Kralik et al., 2014; Stuart et al., 2010). Nevertheless, because of the complexity of the analytical method, few studies using multiple traces have applied Krypton-85 (^{85}Kr) as a main dating tracer. In the present study, the effectiveness of ^{85}Kr as a groundwater dating tracer is evaluated by estimating the age of groundwater using different dating tracers.

In the Kumamoto area, the subject area of the study, an advanced groundwater management policy across administrative boundaries has been highly recognized nationally and internationally, and has been awarded the Japan Water Prize and the “Water for Life” UN-Water Best Practices Award. However, because of emerging concerns about the increasing nitrate and nitrogen levels in groundwater, assessing the age of groundwater is an important task for the empirical assessment of the policy, as well as for sustainable utilization and the sound management and preservation of groundwater.

2. Overview of the study area

2.1. Topographical, geological, and hydrological environment

The subject area of the study, the Kumamoto area, spans 945 km^2 and is situated in southern Japan, where the Shirakawa River originates from Mount Aso and flows from east to west to the Ariake Sea (Fig. 1). Most of the Quaternary deposits in the Kumamoto area are Aso pyroclastic flow deposits, covering the bedrock and andesite and forming a pyroclastic plateau. Although part of the plateau is covered by terrace deposits, the Aso pyroclastic flow deposits that comprise most of the Quaternary deposits (named Aso-1, Aso-2, Aso-3, and Aso-4 in ascending chronological order of eruption) are major units that form the aquifer in the Kumamoto area. The active groundwater circulation in the Kumamoto area displays the hydrogeological characteristics of high permeability, a steep hydraulic gradient of the pyroclastic flow aquifer, and a large amount of precipitation in the Kyushu area. The region is markedly different in terms of the hydraulic gradient of the aquifer and the permeability of component substances from groundwater in the other areas in Japan that are based mainly on aquifers consisting of river alluvial deposits. Lava such as the Togawa lava, the Omine pyroclastic cone, and the Takayubaru lava, and lacustrine deposits, such as the Hanabusa layer and the Futa layer, occur between

pyroclastic flow deposits and were formed during periods when there was no pyroclastic flow activity. The lavas act mainly as aquifers, and the lacustrine deposits act as aquicludes between aquifers. The unconfined aquifer (first aquifer) consists of the lowest part of the lacustrine layer of Aso-4/3 alluvial deposits and Aso-4 above. The depth of this aquifer varies from a few meters to −50 m below the surface in different locations. On the other hand, the confined aquifer (second aquifer) consists of the Aso-1, Aso-2, and Aso-3 pyroclastic flow deposits and the Togawa lava, situated 60–200 m below. These rocks are dense with considerably porous regions and cracks observed around Lake Ezu and near Ukishima and Shimorokka in Kashima. They form a groundwater aquifer with a two-layered structure. The major groundwater resource in the area is dependent on the water intake from this second aquifer. In this study area, previous studies focused on estimation of groundwater age are limited and, furthermore, their results had large uncertainties (Kimura, 1986; Mahara, 1995).

The mean annual temperature and the mean annual precipitation during 1980–2010 in the Kumamoto area were 16.9 °C and 1986 mm, respectively. In addition, precipitation in June and July, the rainy season, accounts for approximately 40% of the annual precipitation.

2.2. Characteristics of local groundwater utilization

The Kumamoto area water supply, which sustains a population of approximately 740,000 inhabitants, is almost 100% dependent on groundwater. The city is therefore known as a groundwater city. Both Kumamoto City and Prefecture actively manage and maintain groundwater resources. They have conducted numerous surveys and studies of the groundwater aquifer structure, maintaining data on groundwater level changes recorded during 20–30 years in as many as 100 groundwater observation wells. However, previous reports have shown a long-term trend of decreasing groundwater levels in every area in the groundwater flow system, from the recharge area to the discharge area, and that the amount of discharge from Lake Ezu, which is fed by a spring, has clearly fallen by 20–30% compared to the level prevailing in the 1950s. However, the total amount of groundwater used in the area is decreasing year-by-year, especially by virtue of water-saving efforts in industrial and agricultural water use. It is difficult to say whether excessive pumping up has lowered the groundwater level and the amount of discharge. Analyses have indicated that the decrease is instead attributable to a decrease in groundwater recharging because of the urbanization of the Kumamoto area and decreased paddy field area resulting from the rice acreage reduction policy (Ichikawa, 2004). In view of those circumstances, the Kumamoto City water works, which use groundwater as source for the tap water supply system and are the largest groundwater consumer in the area, have been alarmed by the long-term decrease of this crucially important water resource. Since 2004, this institution has implemented an active groundwater recharge policy that includes artificial recharging using fallow paddy fields in collaboration with neighboring cities, towns, and villages that possess effective recharge areas. The results have demonstrated that both the groundwater level and the amount of discharge have started to increase (Shimada et al., 2012). This policy can therefore be regarded as a successful case of groundwater management across administrative boundaries. The results have attracted attention: Kumamoto City was awarded the UN Water Best Practices Award in 2013.

2.3. Groundwater flow system of the study aquifer

The distribution of groundwater potential in the second aquifer during the low-water-level season and the high-water-level season is shown in plan view (Fig. 2). The overall groundwater flow system in the area during both seasons consists mainly of two flow lines (A–A' and B–B'). The A–A' line flows from the plateau at the western foot of Aso in the east into the Ariake Sea in the west (Figs. 1 and 2). The B–B' line is a mechanism with a boundary of the area with swollen bedrock at the center of the figure, flowing from the north side to the east side of Mount Kimpo and then toward the Ariake Sea. At the entrance of the B–B' line, there is a confirmed recharge area with high nitrate input where vegetable and livestock farms are highly concentrated (Area C; Hosono et al., 2013).

Moreover, in terms of the groundwater potential in both seasons, the 30-m potential line that is present in the low-water-level season bulges more toward the downstream side in the high-water-level season, exhibiting a large change in the groundwater level. In particular, the groundwater level alters around the lowland in the middle basin of the Shirakawa River by as much as ~15 m. As the aquiclude that divides the unconfined aquifer and the confined aquifer are not present in this area, there is a flow mechanism in which water recharged in the paddy field area around the lowland in the middle basin of the Shirakawa River directly recharges the second aquifer. Subsequently, the groundwater that is recharged in this area flows toward the spring-fed Lake Ezu. Similar groundwater flow systems in the Kumamoto area have been examined in previous studies. One example is the work of Kayane et al. (1987), who used SO_4 ions to show that high-SO_4 groundwater extended from the middle basin of the Shirakawa River to near Lake Ezu. Sulfur of volcanic origin was abundant in the water of the Shirakawa River, and could be used as a tracer. Reportedly, a similar trend was observed in the stable isotope ratio of water. The low isotope ratio of water of Shirakawa River, for which high-altitude Mount Aso is a recharge source, stretched out in the shape of a tongue to near Lake Ezu (Kosaka et al., 2002). As described above, the lowland in the middle basin of the Shirakawa River functions as the major recharge area within the region. There is an active groundwater flow system, in which groundwater that is recharged in this area flows to nearby Lake Ezu.

Additionally, the intervals of potential lines are wider at Lake Ezu and westward (Kumamoto Plain), meaning that the area is a stagnant zone of groundwater flow because of low permeability due to an aquiclude composed of the Ariake clay layer and gentle topography in the plain area.

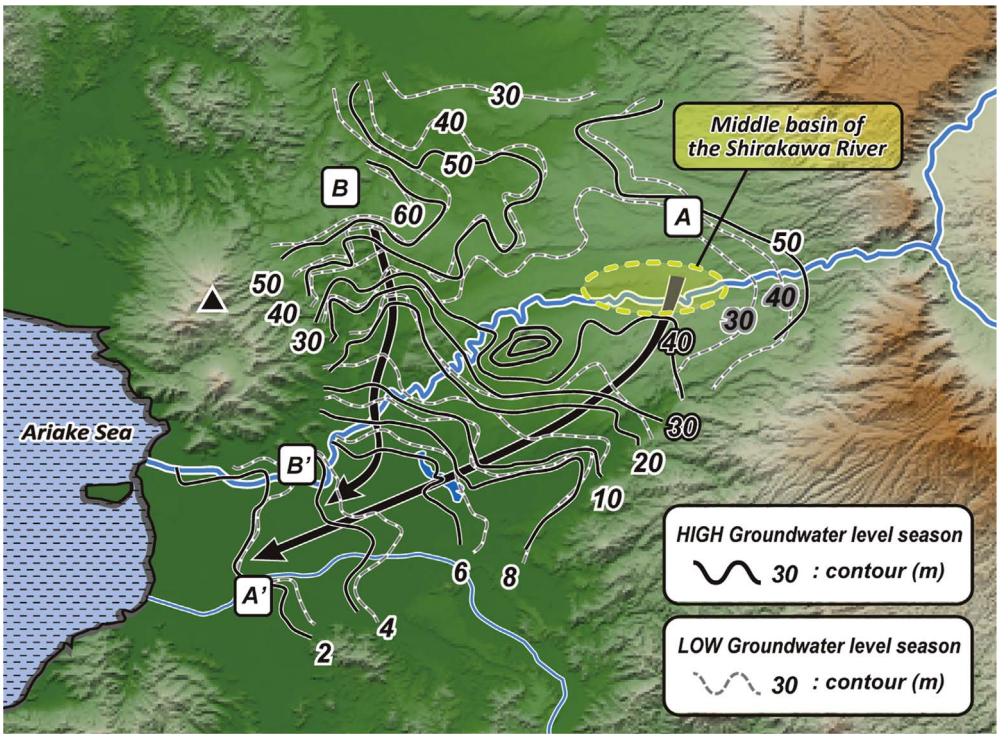

Fig. 2. Groundwater potential distribution in the second aquifer in the low- and high-groundwater-level seasons.

3. Study methods

3.1. Water sampling locations and analysis parameters

Fig. 1 portrays the distribution of the wells and springs from which water was sampled in the present study. There were a total of 41 sampling sites, consisting of 9 sites with shallow groundwater, 22 locations of deep groundwater, and 10 springs. The monitoring wells have a single-screen installed at the certain aquifer and they were selected so that water samples could be collected from different parts of the groundwater flow, from the recharge area to the discharge area and the stagnant zone.

For all locations, the water temperature, electrical conductivity (EC), oxidation–reduction potential (ORP), and dissolved oxygen (DO) were measured on-site. Water samples were brought back to the laboratory for the measurement of stable oxygen and hydrogen isotope ratios. Moreover, young groundwater dating tracers, ^{85}Kr, chlorofluorocarbons (CFCs), sulphur hexafluoride (SF_6), and tritium (^{3}H), were analyzed for 9, 36, 27, and 3 locations, respectively.

The substances ^{85}Kr, CFCs, and SF_6, used here as dating tracers, are all suitable for the measurement of young ages (less than 50 years) because these tracer concentrations have experienced recent increases. It is expected that simultaneous measurement of these dating tracers in the study area will contribute to better dating reliability as well as dating with higher time resolution. However, the field survey of ^{85}Kr was actually conducted in only nine locations, different from the surveys of CFCs and SF_6, which covered the whole area, because the process of Kr gas collection for the measurement of the ^{85}Kr concentration is much more complicated than the process for either CFCs or SF_6. However, considering the groundwater flow system in the area as described above, the sampling locations were selected in the three areas of groundwater recharge, discharge, and the stagnant zone, in two major groundwater flow lines to detect differences in age along the groundwater flow direction.

Information about the classification, location, and well depths of sampling sites and the analytical results are provided in Table 1.

3.1.1. Parameters measured on-site

The water temperature, pH, EC, ORP, and DO were measured on-site. Measurements of the water temperature, pH, EC, and ORP were obtained using one device (D-54; Horiba Ltd.); DO measurements with another one (D-55; Horiba Ltd.). Additionally, during groundwater measurement, these parameters were monitored continuously while water was pumped for at least 30 min so that the water in the well was replaced with surrounding groundwater. The values were read after a sufficient amount of water had been pumped and after the values had become stable.

In addition, water samples were collected in 100-mL plastic bottles for the analysis of stable oxygen and hydrogen isotope ratios.

3.1.2. Laboratory analysis parameters

Stable isotopic (δD, $\delta^{18}O$) analyses were performed in the Isotope Hydrology Laboratory of Kumamoto University in Japan. The

Table 1
Specifications of the sampling sites, measured field parameters, and analytical results.

Classification	Location number	Well Depth (m)	Sampling Date (y/m/d)	On-site measurements					Stable Isotopes		Recharge condition		Age tracers					
				Temperature (°C)	pH	EC (μS/cm)	ORP (mV)	DO (mg/L)	$\delta^{18}O$ (‰)	δD (‰)	Elevation (m)	Temperature (°C)	CFC-12 (pptv)	CFC-11 (pptv)	CFC-113 (pptv)	SF_6 (pptv)	^{85}Kr (Bq/m^3)	^3H (T.U.)
Shallow	SG-1	15	22−07-2012	17.3	7.3	112	305	9.0	−7.55	−47.6	155.9	16.2	1805.0	contam.[b]	1010.9	–		
Shallow	SG-2	40	22−07-2012	20.6	6.8	239	666	11.0	−7.09	−44.9	58.3	16.8	175.3	384.9	92.8	–		
Shallow	SG-3	17	22−07-2012	18.3	7.6	83	348	9.2	−6.37	−39.8	150.0[a]	16.3	311.4	261.7	72.2	–		
Shallow	SG-4	25	22−02-2012	19.1	6.8	204	172	7.8	−7.17	−47.3	144.9	16.3	1153.0	contam.	contam.	15.3		
Shallow	SG-5	–	20−07-2012	20.8	7.2	217	343	7.5	−7.05	−45.9	93.7	16.6	986.7	contam.	contam.	23.7		
Shallow	SG-6	30	21−07-2012	19.1	7.3	206	356	8.1	−7.03	−45.4	75.2	16.7	726.6	contam.	contam.	12.6		
Shallow	SG-7	30	25−07-2012	23.4	7.8	277	560	7.1	−7.43	−47.9	166.8	16.2	159.5	313.2	N.D.	–		
Shallow	SG-8	50	21−07-2012	19.7	8.1	256	−161	0.2	−7.53	−48.4	187.3	16.1	58.9	contam.	contam.	9.1		
Shallow	SG-9	10	10−08-2015	22.0	7.4	312	319	5.2	−6.78	−45.1	65.5	16.7	1421.2	contam.	contam.	11.4	1.430 ± 0.048	
Deep	DG-1	66	22−07-2012	20.7	7.2	236	342	10.6	−7.31	−46.7	122.5	16.4	342.7	contam.	contam.	–		
Deep	DG-2	–	26−07-2012	19.5	6.6	216	302	8.6	−7.60	−49.8	237.2	15.8	97.4	340.7	72.5	–		
Deep	DG-3	–	22−07-2012	19.7	7.2	362	324	8.8	−6.84	−45.0	58.9	16.8	1113.8	contam.	68.1	17.3		
Deep	DG-4	121	04−10-2012	18.5	6.2	236	256	3.1	−6.63	−45.4	76.4	16.7	–	–	–	10.1		
Deep	DG-5	–	26−07-2012	19.7	6.7	172	309	8.3	−7.34	−47.9	169.0	16.2	303.0	1352.3	contam.	–		
Deep	DG-6	–	22−07-2012	20.1	7.3	237	300	7.7	−6.73	−44.3	34.1	16.9	1544.4	4098.9	90.7	–		
Deep	DG-7	82	04−10-2012	17.9	7.5	172	−106	2.5	−6.58	−44.6	46.5	16.8	–	–	–	12.2		
Deep	DG-8	–	25−07-2012	18.3	7.3	160	363	8.3	−6.68	−42.5	150.0[a]	16.3	2577.2	443.7	15.5	4.7		
Deep	DG-9	90	21−07-2012	18.7	6.8	218	396	7.8	−6.75	−47.4	150.3	16.3	1819.4	contam.	contam.	18.9	0.536 ± 0.105	2.1
Deep	DG-10	120	26−07-2012	19.6	7.1	234	288	8.3	−7.05	−45.6	81.1	16.6	266.2	contam.	contam.	–		
Deep	DG-11	54	21−07-2012	18.1	7.2	190	351	8.7	−7.31	−47.2	141.0	16.3	–	–	–	6.1		
Deep	DG-12	71	31−10-2012	18.7	6.7	237	401	7.4	−7.05	−49.7	233.8	15.8	1928.1	contam.	contam.	18.0		
Deep	DG-13	–	20−07-2012	20.2	6.3	201	381	8.7	−7.25	−46.3	109.8	16.5	1405.5	contam.	contam.	10.1		
Deep	DG-14	–	29−06-2012	19.5	6.7	230	171	7.0	−7.32	−47.7	160.3	16.2	1030.8	contam.	contam.	18.2	0.067 ± 0.014	1.9
Deep	DG-15	60	04−10-2012	18.3	7.7	185	279	1.6	−7.58	−49.6	229.1	15.8	–	–	–	8.5		
Deep	DG-16	117	04−10-2012	17.5	8.5	128	223	1.4	−7.39	−48.1	173.7	16.1	–	–	–	7.3		
Deep	DG-17	145	26−06-2012	21.4	8.4	1315	−283	0.3	−6.81	−45.1	62.6	16.7	N.D.	14.5	N.D.	2.1	N.D.	N.D.
Deep	DG-18	135	13−09-2014	18.2	6.9	188	156	7.3	−7.06	−45.5	79.1	16.7	N.D.	N.D.	N.D.	N.D.	N.D.	
Deep	DG-19	81	11−09-2014	17.3	7.5	130	149	7.1	−7.52	−46.8	126.0	16.4	N.D.	N.D.	N.D.	N.D.	N.D.	
Deep	DG-20	100	15−09-2014	20.7	8.0	426	−190	0.0	−7.08	−47.0	135.1	16.4	N.D.	N.D.	N.D.	N.D.	N.D.	
Deep	DG-21	145	07−08-2015	21.0	8.2	224	234	4.2	−6.86	−45.8	89.9	16.6	contam.	contam.	contam.	11.2	0.415 ± 0.017	
Deep	DG-22	150	12−08-2015	18.8	8.0	144	292	6.6	−7.05	−47.2	141.4	16.3	contam.	contam.	70.8	11.0	0.212 ± 0.011	
Spring	Sp-1		20−04-2012	16.1	7.3	80	247	6.4	−7.11	−45.2	69.3	16.7	370.3	454.8	83.4	7.7		
Spring	Sp-2		19−04-2012	14.3	7.7	78	259	7.1	−7.80	−48.9	204.1	16.0	190.8	258.8	79.2	–		
Spring	Sp-3		19−04-2012	13.3	7.6	69	259	8.4	−8.26	−51.2	290.3	15.5	262.1	188.6	54.1	–		
Spring	Sp-4		19−04-2012	16.8	7.1	100	265	8.8	−7.42	−46.8	128.1	16.4	296.6	395.6	81.4	–		
Spring	Sp-5		18−04-2012	16.8	6.7	105	270	8.3	−7.37	−46.5	117.7	16.4	264.8	272.5	contam.	9.0		
Spring	Sp-6		20−07-2012	17.7	7.3	135	342	8.3	−7.39	−46.3	108.4	16.5	731.8	822.0	contam.	–		
Spring	Sp-7		19−04-2012	17.2	6.9	132	254	7.1	−7.26	−46.2	103.7	16.5	1587.1	contam.	contam.	8.8		
Spring	Sp-8		21−04-2012	18.9	6.8	217	257	7.3	−7.31	−46.3	107.9	16.5	973.7	2165.6	contam.	7.1		
Spring	Sp-9		19−04-2012	16.2	7.7	254	251	6.8	−8.06	−51.0	282.4	15.5	318.6	285.2	82.8	9.2		
Spring	Sp-10		19−04-2012	16.6	6.7	200	240	6.0	−6.79	−43.9	18.5	17.0	605.4	736.9	107.5	–		

[a] Convenience value. Due to the large δD value, the estimated recharge altitude becomes lower than that of sampling elevation.
[b] Contam. represents the significantly high concentration or cannot detected due to the waveform turbulence during analysis.

hydrogen and oxygen isotopic ratios are expressed as relative differences (δ values) from Standard Mean Ocean Water (SMOW) in parts per mil (‰). The $\delta^{18}O$ and δD were measured by a mass spectrometer (DeltaV; Thermo Electron Corp.) referenced to the Vienna Standard Mean Ocean Water (VSMOW). The accuracy of the measured value is within ± 0.50‰ for δD and within ± 0.05‰ for $\delta^{18}O$.

3.1.3. Dating tracers

The dating tracers used in the present study are ^{85}Kr, SF_6, CFCs, and ^{3}H. The history of the concentration level of each tracer is depicted in Fig. 3. The characteristics and analytical methods for the dating tracers are described below.

3.2. Analytical methods for dating tracers

3.2.1. ^{85}Kr

The tracer ^{85}Kr is a radioactive isotope of the noble gas krypton with a half-life of 10.76 years (Seelmann-Eggebert et al., 1981). A low natural background concentration of ^{85}Kr is produced by spallation and (n, γ) reactions of cosmic neutrons with the stable isotope ^{84}Kr. Almost all ^{85}Kr in the environment is of anthropogenic origin, mainly released from spent nuclear fuel reprocessing plants operating in the northern hemisphere since the 1940s (Winger et al., 2005). The isotope is a fission product of uranium and plutonium: emissions of ^{85}Kr are directly related to plutonium production (Schroder and Roether, 1975). A constant concentration of stable Kr in the atmosphere (1.14 ppm) allows the use of $^{85}Kr/Kr$ specific activity as a dating ratio that is independent of both the recharge temperature and excess air trapped during recharge. Furthermore, the ratio is not sensitive to partial sample loss during either sampling or analysis (Cook and Solomon, 1997).

The ^{85}Kr concentrations adopted in this study are depicted in Fig. 3, together with those reported by other researchers (Alikhani et al., 2016; Aoyama et al., 2008; Cauwels et al., 2001; Loosli, 1992; Loosli et al., 2000; Momoshima et al., 2010; Okai et al., 1984; Stockburger et al., 1977; Tomášek and Wilhelmova, 1997; Wilhelmová et al., 1990; Winger et al., 2005; Visser et al., 2015).

Groundwater age dating using ^{85}Kr is limited because of its complicated measurement procedures. Furthermore, because the radioisotope ^{85}Kr has an extremely low concentration in groundwater, an effective Kr extraction system from a large volume of groundwater (10^4 L) is required in this study. Recently, Ohta et al. (2009) developed a Kr extraction system from groundwater samples using an external inflow-type hollow-fiber membrane that was designed to be applicable to on-site sampling. In this study, the gas-extraction system was improved from that reported by Ohta et al. (2009). The vacuum pump was inserted into the vacuum desiccator, which was initially filled with pure nitrogen, to avoid mixing with modern Kr in present-day air.

To estimate the groundwater age from ^{85}Kr in groundwater, three steps were necessary: Step 1, on-site extraction and collection of dissolved gases in groundwater; Step 2, on-site separation of Kr gas from other dissolved gases; and Step 3, measuring the ^{85}Kr concentration in the laboratory (Fig. 4).

The gas-extraction system was mounted on a small truck. A groundwater sampling pump (MP-1; Grundfos Co.) run by three parallel AC

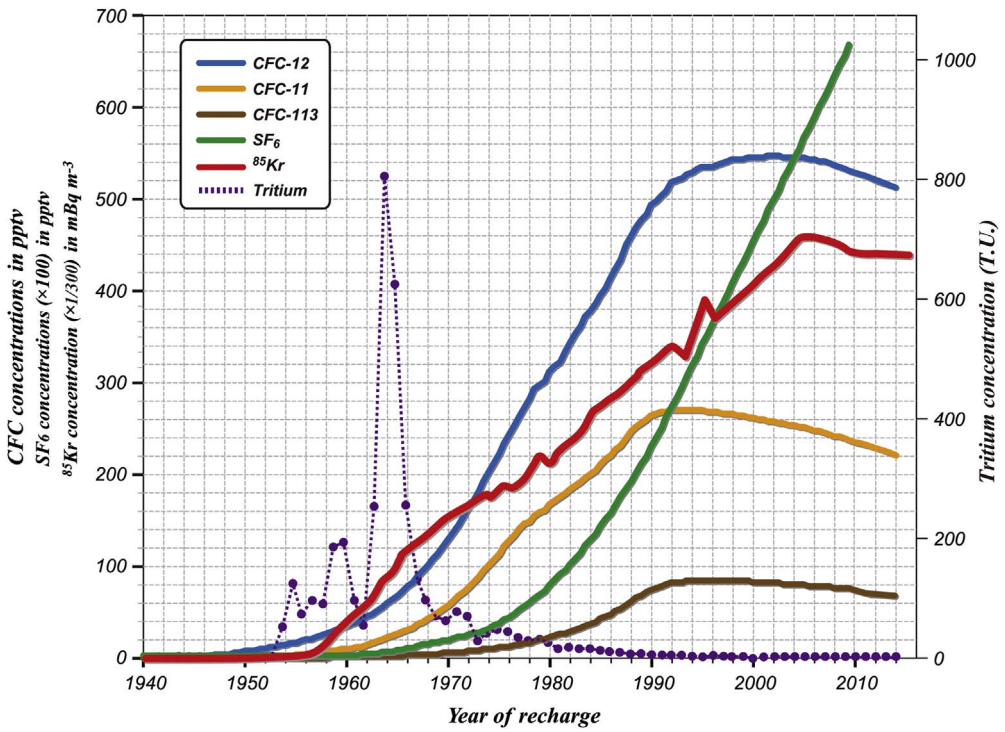

Fig. 3. Concentration of chlorofluorocarbons (CFCs), SF_6, and ^{85}Kr in the atmosphere and of tritium in rainfall.

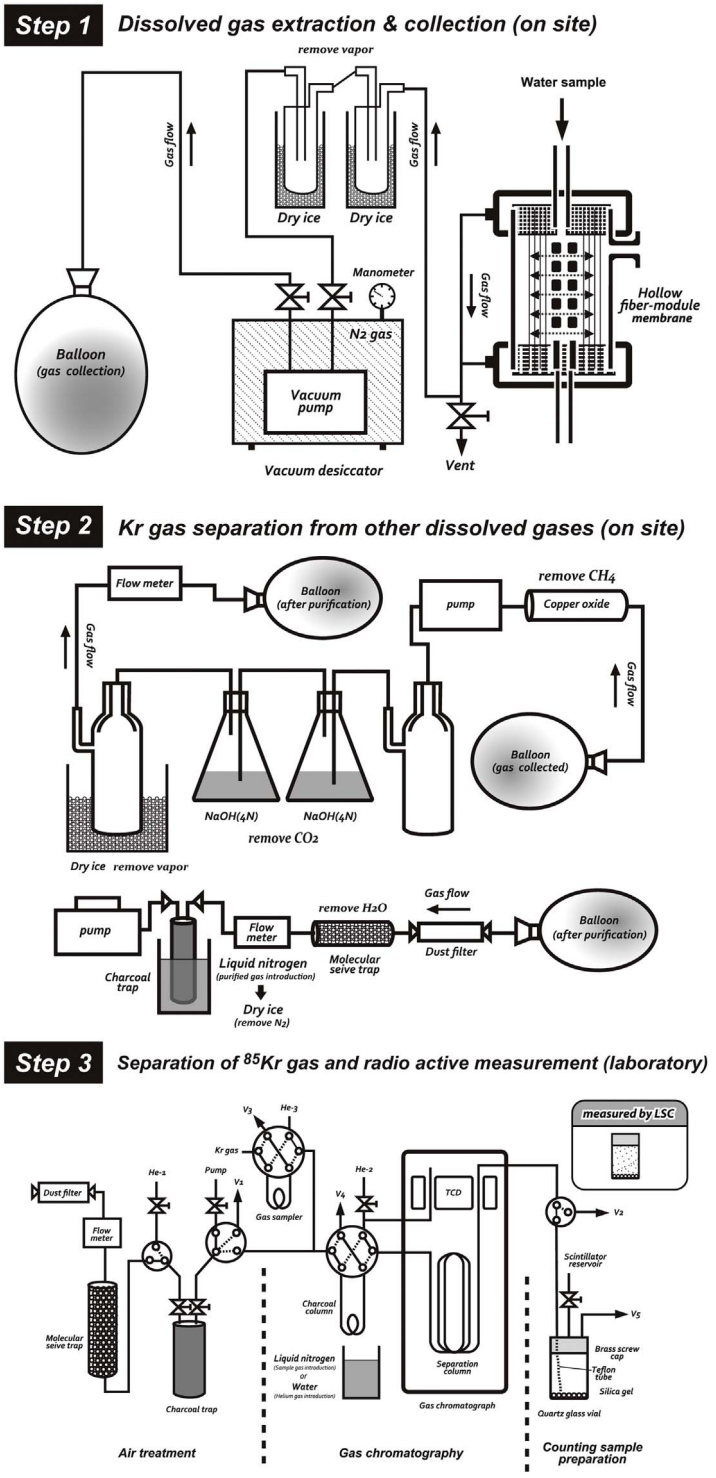

Fig. 4. Procedure for measurement of the ^{85}Kr concentration.

generators was used to collect the water. Dissolved gases in groundwater were extracted at the groundwater-sampling well site by running through a volume on the order of 10^4 L of groundwater. The extracted gases were collected into a 1000-Lrubber balloon (Step 1). Subsequently, the gas was purified on-site with copper oxide heated at 600 °C, a NaOH solution, and a dry-ice trap to remove CH_4, CO_2, and H_2O, respectively. The purified gases were transferred to a charcoal trap consisting of a stainless cylinder cooled at liquid N_2 temperature. Most of the N_2 in the charcoal trap was released at dry-ice temperature, then carried back to the laboratory (Step 2). In the laboratory, Kr gas

was separated from residual gases using gas chromatography. The Kr gas was transferred to a quartz glass vial under liquid N_2 temperatures with addition of a *p*-xylene-based scintillator cocktail for LSC measurements. The radioactivity of ^{85}Kr was measured with a low-level liquid scintillation counter; LB-5 by ALOKA Co. (Momoshima et al., 2011; Step 3). Groundwater can be dated up to 0.5 years because of very low detection limit of the counting system, 0.0015 Bq (Momoshima et al., 2011).

3.2.2. CFCs and SF_6

The atmospheric trace gases CFC-11, CFC-12, CFC-113, and SF_6 are increasingly being used as tracers of the groundwater age (IAEA, 2006; USGS, 2016). Large-scale production of CFC-12 began in the early 1940s, with CFC-11 production subsequently commencing in the 1950s. CFC-11 and CFC-12 were used mainly for refrigeration and air-conditioning; CFC-113 was used as a solvent. Eventually, these compounds leaked into the environment and their atmospheric concentration rose until the 1990s, when, to protect the ozone layer, production was cut back as a result of the Montreal Protocol. SF_6, another industry-derived gas, has been detectable in the atmosphere since the early 1960s: its concentration is still rising strongly.

Groundwater samples for CFC analysis were collected in triplicate and stored in glass bottles sealed with metal-lined caps (Busenberg and Plummer, 1992). We analyzed the CFCs using a closed system purge and trap gas chromatography with an electron capture detector (GC-8A; Shimadzu Corp., Japan). The values were reported only if the concentrations of at least two measurements were within 10% for concentrations higher than 100 pg/kg. For concentrations below 100 pg/kg, values were reported only if at least two measurements were within 20 pg/kg of each other (Johnston et al., 1998). The analytical uncertainty associated with CFC analysis was less than 3%.

The collection procedure for SF_6 analysis is fundamentally identical to that used for CFCs, but the volume of glass bottles for SF_6 collection (500 mL) is greater than that of CFCs (125 mL) because of the low dissolved concentration in water. The analytical procedure is similar to that for CFCs, but the details of the SF_6 analytical procedure used here follow Busenberg and Plummer (2000) of the U.S. Geological Survey. The analytical uncertainty associated with the SF_6 analysis was less than 5%.

3.2.3. Tritium

Historically, ^3H (tritium), a radioisotope of hydrogen, has been the most widely used tracer of young groundwater. As tritium has a half-life of 12.34 years, and because it generally behaves conservatively, the tritium content of water is a reliable indicator of groundwater age. Numerous studies of groundwater age have been conducted over the years using ^3H (Begemann and Libby, 1957; Egboka et al., 1983; Nir, 1964; Shevenell and Goff, 1995; Simpson and Carmi, 1983; Vuataz and Goff, 1986). In these studies, the hypothesis is that the historical ^3H bomb concentration (bomb peak) recorded in the 1960s is conserved during groundwater flow and is the key indicator for groundwater age estimation. However, unlike CFCs and SF_6, the ^3H concentration in precipitation has declined exponentially since the cessation of thermonuclear atmospheric testing in the 1960s (Yabusaki et al., 2003; Fig. 3), resulting in its current low activity in groundwater and difficulty in detecting the key indicator “bomb peak.”

Measurement of ^3H was performed using a liquid scintillation counter (TRI-CARB2750TR/LL; PerkinElmer Inc., USA) subsequent to electrolytic enrichment. Results are reported as tritium units (T.U.), i.e., one atom of ^3H in 10^{18} atoms of hydrogen, with a maximum error of 0.3 T.U.

4. Results and discussion

4.1. Analytical results of dating tracers

4.1.1. ^{85}Kr

For estimation of the groundwater age with ^{85}Kr, the apparent age was estimated using the procedure described below.

First, a liquid scintillation counter was used to determine the radioactivity of ^{85}Kr extracted from dissolved gases in groundwater using the method described in Section 3.2.1. A background (BG) sample was prepared with the same *p*-xylene based scintillator as the ^{85}Kr samples and measured alternately with the ^{85}Kr sample. A paired measurement (^{85}Kr/BG for 500 min each) was carried out at least 10 times at adequate intervals to check for Rn contamination. The net count rate (cps) of the ^{85}Kr sample was obtained by subtracting the BG count rate (cps) using only paired data (^{85}Kr/BG) without Rn contamination.

The net count rate of the sample was then converted to the atmospheric ^{85}Kr concentration (Bq/m^3) using Eq. (1):

$$\frac{\text{Net count rate of sample (cps)} \times 1.14\ (\text{atmospheric Kr mL}/\text{m}^3)}{\text{Volume of Kr of sample (mL)} \times \text{Counting efficiency of } ^{85}\text{Kr}} \quad (1)$$

It is possible to confirm that no contamination with Rn occurred by checking the stability of the count rate of the ^{85}Kr sample with time. After the complete decay of Rn, the count rate of the ^{85}Kr sample stabilizes, showing rather constant counts with time even if Rn contamination occurred during sampling.

The error was calculated using Eq. (2):

$$\sqrt{\left(\frac{\text{Count rate of } ^{85}\text{Kr sample}}{\text{Total counting time of } ^{85}\text{Kr sample}}\right) + \left(\frac{\text{Count rate of BG sample}}{\text{Total counting time of BG sample}}\right)} \quad (2)$$

In addition, the atmospheric ^{85}Kr concentration (Bq/m^3) on the day of measurement was decay-corrected to the day of groundwater sampling and compared with the historical trend of atmospheric ^{85}Kr concentration. Subsequently, the apparent age was estimated.

The atmospheric ^{85}Kr concentration in the study area was 1.443 Bq/m^3 ± 0.068 (n = 2) in 2015 using the method described above, which is similar to 1.432 Bq/m^3 of the Northern hemisphere in 2014 (Visser et al., 2015).

In this study, based on the local groundwater flow system, the ^{85}Kr concentration was measured at three locations in each of Lines A–A' and B–B', corresponding to the recharge area, the discharge area, and the stagnant zone of groundwater. In the A–A' line, the concentrations were 0.536 ± 0.105 Bq/m^3, 0.067 ± 0.014 Bq/m^3, and below the limit of detection, respectively. These values were converted into the apparent age when assuming the piston-flow model, yielding results of approximately 16 ± 1.8 years (DG-9), 36 ± 1.2 years (DG-14), and not less than 55 years (DG-17), respectively. These values are consistent with the local groundwater flow system, in which the groundwater age increases from the recharge area to the discharge area. In the B–B' line, concentrations below the limit of detection were measured in all locations (DG-18, 19, and 20) indicating that the apparent age was not less than 55 years in this groundwater flow line. In Area C, the concentrations were 1.430 ± 0.048 Bq/m^3 in the shallow groundwater and 0.415 ± 0.017 and 0.212 ± 0.011 Bq/m^3 in the deep groundwater; the corresponding apparent ages were approximately 1 ± 0.7 year (SG-9), 20 ± 0.5 years (DG-21), and 31 ± 0.5 years (DG-22), respectively (Fig. 5).

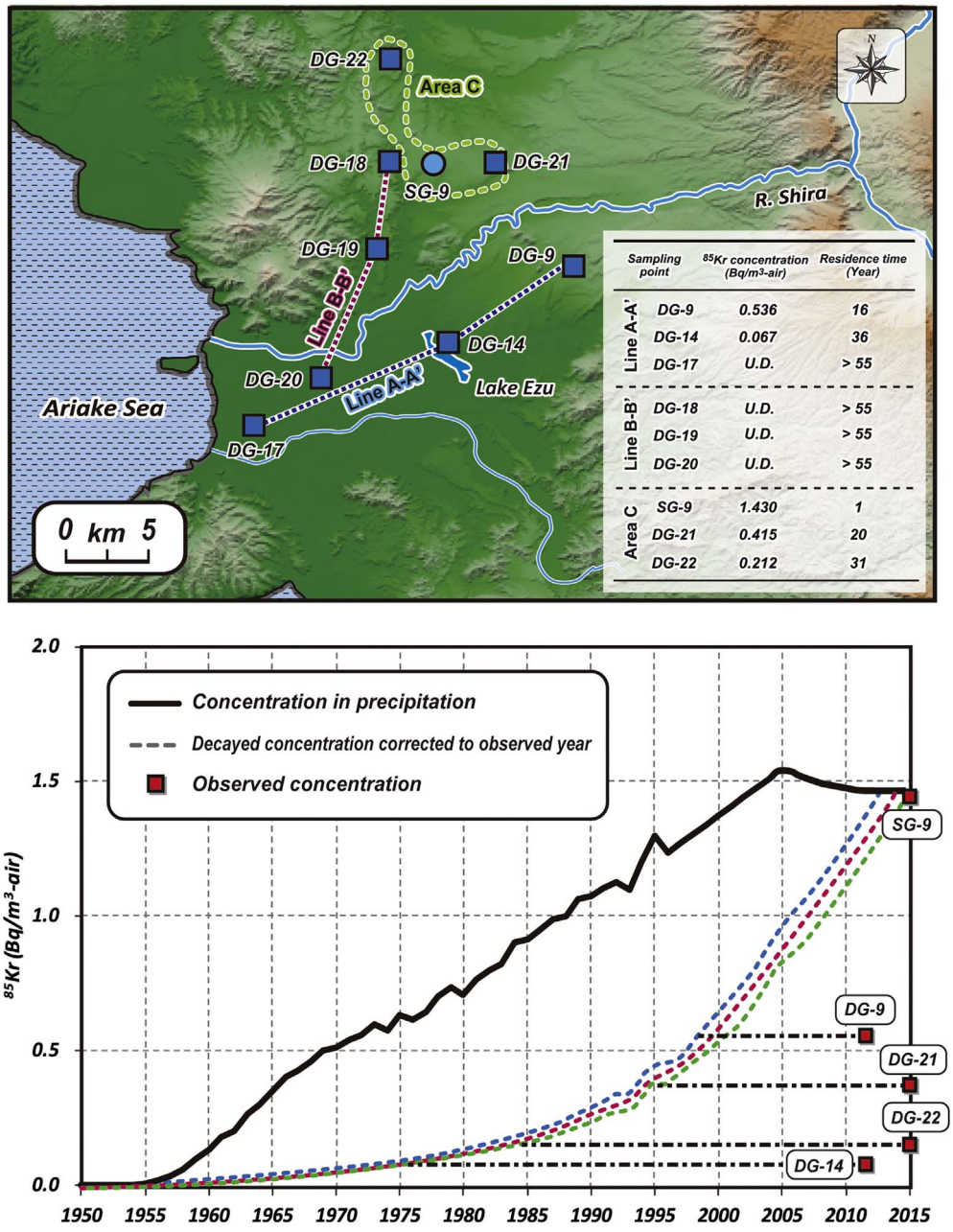

Fig. 5. ^{85}Kr concentration at nine sampling locations and estimated mean residence time.

4.1.2. CFCs, SF_6

To compare groundwater and atmospheric concentrations, the CFCs and SF_6 values in groundwater were converted to the equivalent atmospheric concentration (EAC) at the time of recharge, based on Henry's Law.

$$\mathrm{EAC\ (pptv)} = \mathrm{CFCs_{gw}}/\{K_{\mathrm{CFCs-H}} \times (P - P_{\mathrm{H2O}}) \times 100\} \quad (3)$$

$$\mathrm{EAC\ (pptv)} = \mathrm{SF_{6gw}}/\{K_{\mathrm{SF6-H}} \times (P - P_{\mathrm{H2O}}) \times 100\} \quad (4)$$

where EAC denotes the equivalent atmospheric concentration (pptv); $\mathrm{CFCs_{gw}}$ corresponds to the concentration of dissolved CFCs in groundwater (p mol/L); $K_{\mathrm{CFCs-H}}$ denotes the Henry's Law constant for CFCs; $\mathrm{SF_{6gw}}$ represents the concentration of dissolved SF_6 in groundwater (f mol/L); $K_{\mathrm{SF6-H}}$ is the Henry's Law constant for SF_6; P is the total atmospheric pressure; and P_{H2O} is the water vapor pressure. In this calculation, the parameters of average temperature and average elevation (barometric pressure) are those of the sites at which the groundwater samples were collected (IAEA, 2006).

In this study, to estimate the altitude of recharge, springs and river water with geographically limited catchment obtained in the study area were selected at multiple altitudes to obtain the linear approximation of the relation between altitude and the δD value of recharged groundwater (recharge water line; Kazahaya and Yasuhara, 1994). The calculated recharge water line in the Kumamoto area is expressed by the following equation:

$$\delta D_r = -0.0270H - 43.372. \quad (5)$$

where δD_r is the δD value of recharged groundwater and H is the altitude (m).

Moreover, assuming that the recharge temperature is equal to the groundwater temperature at the recharge altitude, the recharge temperature was calculated from the recharge altitude obtained from equation (4) using the typical common local air temperature lapse rate of −0.55 °C/100 m (Yoshino, 1986).

Using the parameters of the recharge altitude and the recharge temperature obtained as described above, the EAC value was obtained for CFCs and SF_6. Additionally, although three types of CFCs (CFC-11, CFC-12, and CFC-113) were analyzed, only CFC-12 is described in the discussion below because it is the most stable one in the underground environment (Plummer et al., 1998).

The EAC values of groundwater and spring water are displayed with respect to the different local land-use categories (Fig. 6). The historical trend of the concentration of CFCs and SF_6 in the northern hemisphere is also illustrated in the figure.

The EAC values of groundwater and spring water varied widely. There also were many locations for which dating could not be performed because the value was higher than the peak atmospheric concentration and therefore could not be compared with it; this phenomenon was more apparent for SF_6. In terms of land use, the concentration tended to be significantly higher in urban areas, including industrial areas. However, although no notable increase in the concentration was detected in forests and farmland, there

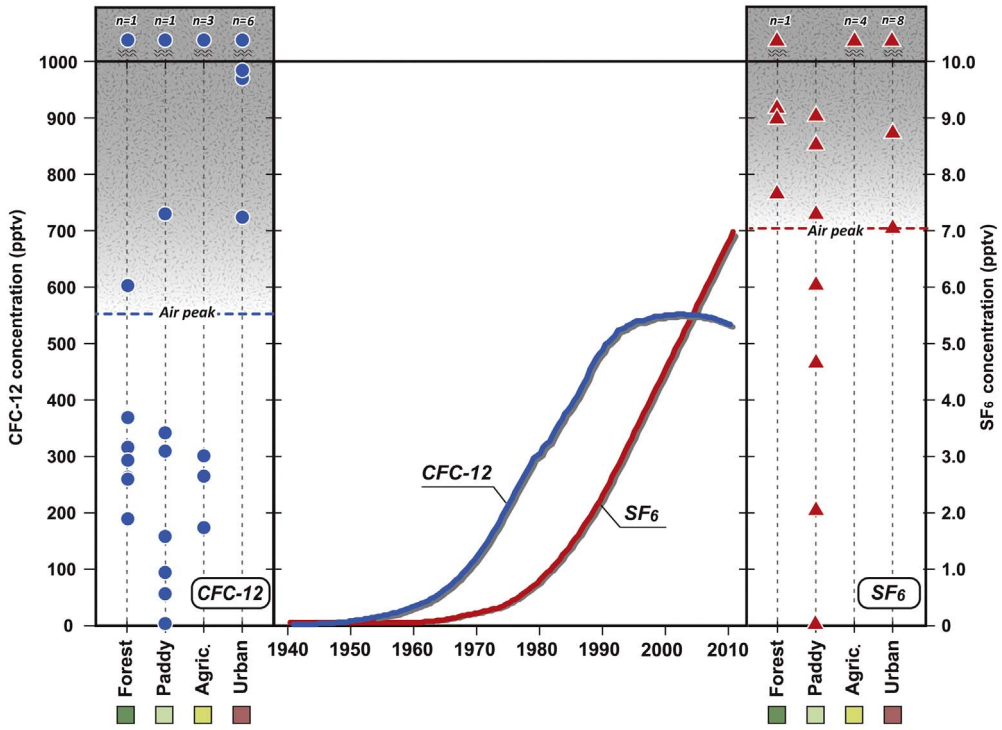

Fig. 6. Equivalent atmospheric concentration (EAC) values of groundwater and spring water for CFC-12 and SF_6 in different land-use types. The atmospheric concentration is also plotted.

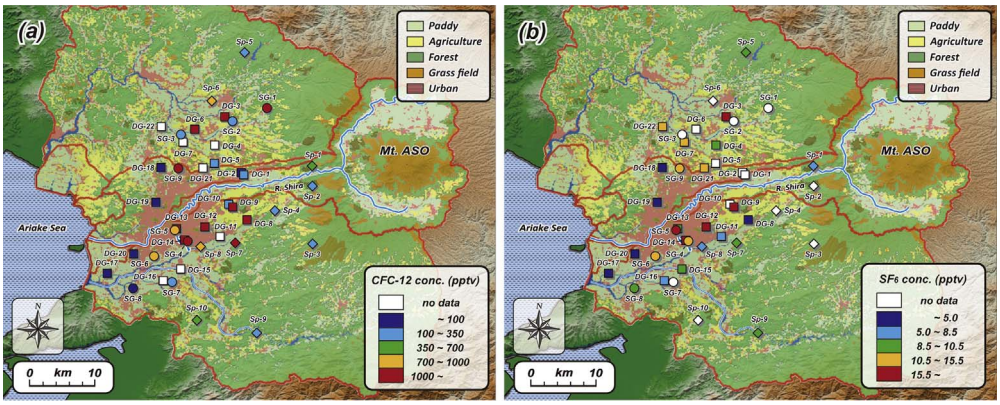

Fig. 7. Plan view of (a) CFC-12 concentration and (b) SF_6 concentration plotted on the local land-use pattern.

were locations above the atmospheric concentration peak in all land-use types of the studied area. This trend is readily apparent in the plan view of the distribution shown over the local land-use map in Fig. 7.

Regarding the elevated concentration of CFCs, anthropogenic effects from urban and industrial areas are suspected to be a generally possible source (IAEA, 2006). For the elevated SF_6 concentration, the local geology in this area is a possible source. Koh et al. (2007) reported underestimation of SF_6 ages compared with CFCs for samples collected at Jeju Island, Korea. In addition, Heilweil et al. (2009) described the difficulty of age dating using SF_6 in a volcanic area because of the excess SF_6 derived from volcanic rocks. These findings confirm the difficulty of age dating by SF_6 in aquifers containing volcanic deposits, such as those in the Kumamoto area.

Although similar trends were observed in the concentration distribution of both tracers of CFCs and SF_6, it was difficult to judge the extent of artificial or terrestrial addition to the concentration based on land-use patterns. The results show that it was difficult to estimate the age by application of the dating tracers CFCs and SF_6 in the study area.

4.2. Validity of estimated groundwater age

4.2.1. Groundwater flow in the A-A' line

Validity of groundwater age was performed using ^3H in the three locations along the A–A' line corresponding to the recharge area (DG-9), the discharge area (DG-14), and the stagnant zone (DG-17) of groundwater, which were the same places for the measurement of the ^{85}Kr concentration.

Firstly, in order to judge the groundwater flow model, TRACERMODEL1 (Böhlke, 2006) were adopted. Böhlke (2006) described the groundwater flow concepts of four models; the piston flow model (PFM), exponential mixing model (EMM), exponential piston flow model (EPM), and binary mixing model (BMM). Three results obtained from analysis of environmental tracers (^3H and ^{85}Kr) along the A–A' line (DG-9, DG-14 and DG-17) are compared with those of the models shown in Fig. 8. From the analytical results in Fig. 8, sample in the recharge area (DG-9) was plotted on EPM line, whereas the discharge area (DG-14) was plotted on PFM line. The mean groundwater ages as judged from the figure were approximately 24 years (DG-9) and 37 years (DG-14).

Next, based on this defined groundwater flow model estimated by TRACERPLOT1, the LUMPED model (Ozyurt and Bayari, 2003) were adopted to evaluate groundwater age. Repeated data of ^3H concentration at the same location are useful as time-series information of ^3H in each location, which are the input data for the LUMPED model analysis (Ozyurt and Bayari, 2003). The previous measured ^3H values were reported in the three locations (Kumamoto prefecture and Kumamoto city, 1995; Mahara, 1995).

To determine the mean age of groundwater by the LUMPED model, the conceptual models of groundwater system and the temporal variation of the measured environmental tracer input concentration are needed. The measured tracer input concentration, *Cinput(t)*, is used to calculate the tracer output concentration, *Coutput(t)*, which, in turn, is compared with the concentrations measured in the output from the system. The relationship between input and output concentrations is described by the following convolution integral (Maloszewski and Zuber, 1982):

$$C_{output}(t) = \int_0^\infty C_{input}(t - t')\exp(-\lambda t')\, g(t')\, dt' \tag{1}$$

where (t-t') is the time of entry, t' is the travel time, and λ is the decay constant of radioactive tracers. The weighting function $g(t')$ describes the output distribution of a conservative tracer instantaneously infected in the water entering the system. The mean groundwater age T for the PFM is expressed as follows;

$$g(t') = \delta(t - t') \tag{2}$$

$$T = V_p / Q_p \tag{3}$$

where δ is Dirac delta function.

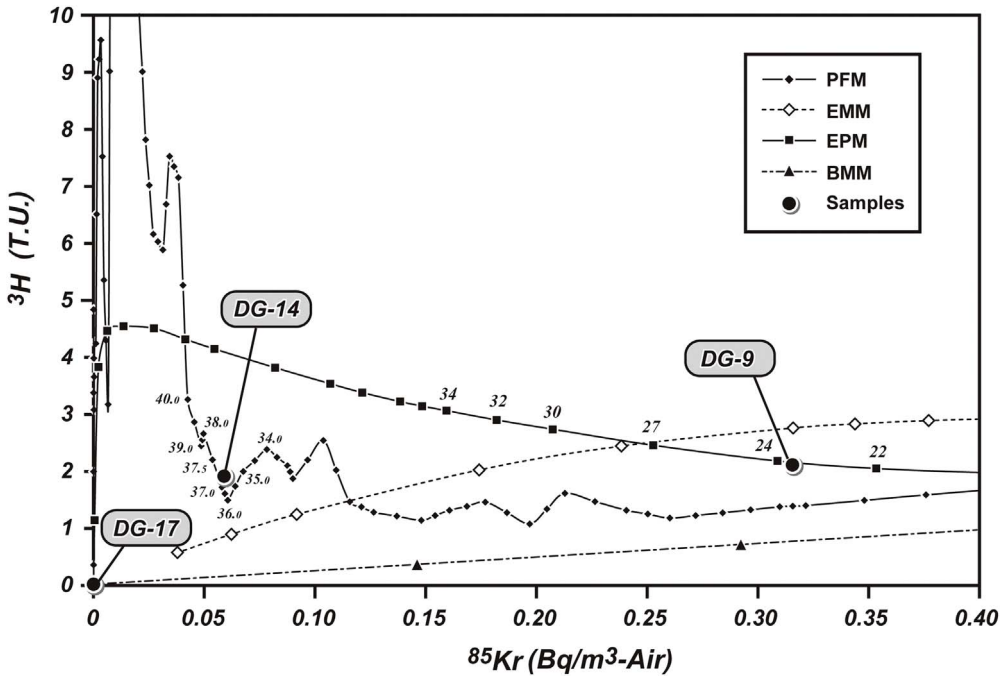

Fig. 8. Comparison between measured ^{3}H and ^{85}Kr concentrations with the model curves.

For the EPM is expressed as follows;

$$g(t') = \left(q_m/(q_m + q_p)\right)^2 * \left((V_m + V_p)/V_m\right) * exp\left(-(q_m/V_m) * t\right) \quad (4)$$

$$T = (V_m + V_p)/(q_m + q_p) \quad (5)$$

where q_m is the groundwater flux with a mixing (exponential-flow) component (m^3/year); q_p is the groundwater flux with no mixing (piston-flow) component (m^3/year); V_m is the volume of groundwater flux with a mixing (exponential-flow) component (m^3); and V_p is the volume of groundwater flux without a mixing (piston-flow) component (m^3).

When the weighting function $g(t')$ is used express the repeated measurements of ^{3}H concentration by fixing each parameter, the estimated mean age of the targeted groundwater indicates the actual groundwater flow conditions. Thus, the estimation of each parameter of Eq. (4) is limited by measurement, and the accuracy of $g(t')$ is dependent on the number of measured values. The mean groundwater age T is defined once each parameter has been fixed.

The parameter configuration required for the LUMPED model analysis in this study is explained below. First, the catchment of each location was set based on the groundwater equipotential map in the high-water-level season (Fig. 2). For water storage (V_m and V_p), the total aquifer storage was calculated by setting the groundwater reservoir volume from the catchment area size obtained with Arc GIS considering the depth of the water-collecting wells and assuming that the effective porosity was constant at 0.2 (Kayane, 1980). In addition, as for the recharge flux ($q_m$and q_p), the mean value of precipitation in Kumamoto for 1971–2000 (P; 1992 mm) was used. It was assumed that 900 mm of the precipitation was lost as a result of evapotranspiration and surface runoff; the remainder permeated underground to recharge the groundwater. However, accurate determination of the recharge and storage amounts that were involved in circulation was extremely difficult because of the complicated groundwater flow system. Therefore, ± 20% of the recharge and storage amounts estimated as described above were set as the initial values for calculation as shown in Table 2. The parameters were determined in an attempt to select the optimal value in the range. However, because there were a limited number of measured values, the resulting groundwater age could not be narrowed down to a single value; therefore, there was an error range for the estimation result value.

The parameters and their mean groundwater ages in different locations are presented in Table 2. The results indicated that the mean groundwater age was 26–35 years with EPM in the recharge area (DG-9), and 36 years with PFM in the discharge area (DG-14; Fig. 9). The mean groundwater age could not be estimated in the stagnant zone (DG-17) because the ^{3}H concentration was not detected, although it was determined to be at least 50 years considering its half-life. The mean groundwater ages estimated by 2-tracer model (TRACERMODEL1) and time series of ^{3}H analysis (LUMPED model) showed good agreement in this study.

The traveling time between the recharge area and the discharge area was calculated as 6–12 years in the present study assuming a straight flow-line connection from the recharge to discharge area. This traveling time suggests a flow rate of 625–1250 m/year, which is quite fast compared to other fields: that in Carrizo Sand, Texas was 1.6 m/year obtained by the ^{14}C method (Pearson and White, 1967); the value in the Nubian Aquifer (Egypt) was 2.0 m/year using the ^{81}Kr method (Sturchio et al., 2004); and that in the confined

Table 2
Repeated measurement values of ^{3}H, parameters for the LUMPED model, and estimated residence times.

Location number	GW flor model	^{3}H concentration (T.U.)					Parameters for LUMPED model				Ratio of each component (%)		Estimated residence time (year)	Residence time by ^{85}Kr (year)
		This study	June, 1993	Dec., 1989	Nov., 1974	June, 1974	Recharge amount (10^6 m3/year)		Reservoir volume (km^3)					
							Min.	Max.	Min.	Max.	PFM	EM		
DG-9	EPM	2.1	7.8				2.6	3.8	0.083	0.125	35–43	57–65	26–35	16
DG-14	PFM	1.9	5.2	9.2	4.3	3.4	3.6	5.4	0.130	0.194	100	–	36	36
DG-17	–	N.D.	N.D.										> 50	not less than 55

aquifer in Florida was 7.0 m/year from the ^{14}C method (Hanshaw et al., 1965). The relatively rapid groundwater circulation in this study may result from the hydrogeological characteristics, which include high permeability, the steep hydraulic gradient of the pyroclastic flow aquifer, and the large amount of precipitation in this study area. The fact that the nitrate concentration in groundwater decreased along the flow direction due to dilution of the Shirakawa river water was confirmed by Hosono et al. (2013) from $\delta^{15}N$–data. This decrease of nitrate concentration is a result of the high groundwater circulation in this area. Thus, there is a potential risk of the drinking resource being exposed to problems once groundwater contamination occurs.

4.2.2. Groundwater flow in the B–B' line

There has been only one previous study to estimate the groundwater age in this flow line using the ^{3}H method (Kimura, 1986). The groundwater in this area was stagnant-type and the ratio of ^{3}H-free water was 62–92%. The concentrations of CFCs, SF_6, and ^{85}Kr were lower than the detection limit in this study, reflecting the relatively longer age of groundwater and in good agreement with the findings of the previous study. The occurrence of denitrification is suggested by the results of the nitrate analysis (concentration and $\delta^{15}N{-}NO_3$ values) and DO values (Hosono et al., 2013). Recent studies have verified that the groundwater age is a primary controlling factor of the denitrification process: old groundwater is strongly affected by the process (Green et al., 2009; Ocampo et al., 2006; Seitzinger et al., 2006). Hence, the groundwater with the longer age in this area detected in the present study supports the existence of this denitrification phenomenon.

4.2.3. Area C

Three samples from Area C, with a high nitrate input, had a long-term record of NO_3^-–N concentration because these samples were obtained from regional water supply wells at which the quality is monitored periodically (Fig. 10).

Fig. 11 focuses on the monthly record of NO_3^-–N concentration in the most recent five years. The NO_3^-–N concentration in the

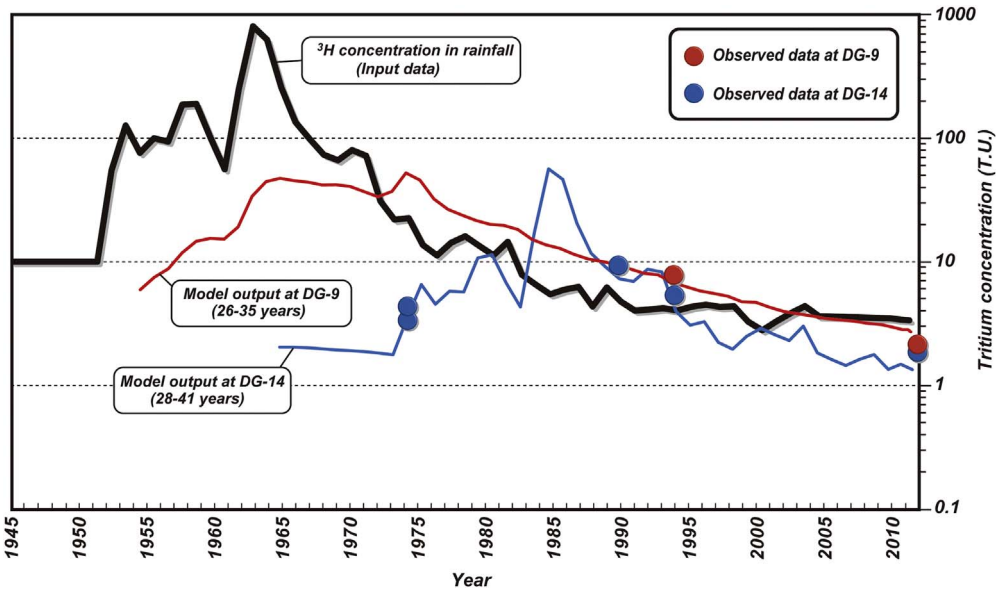

Fig. 9. Comparison of observed and model output ^{3}H concentrations. Although several optimal model outputs were estimated, only one example is plotted for each location in this figure.

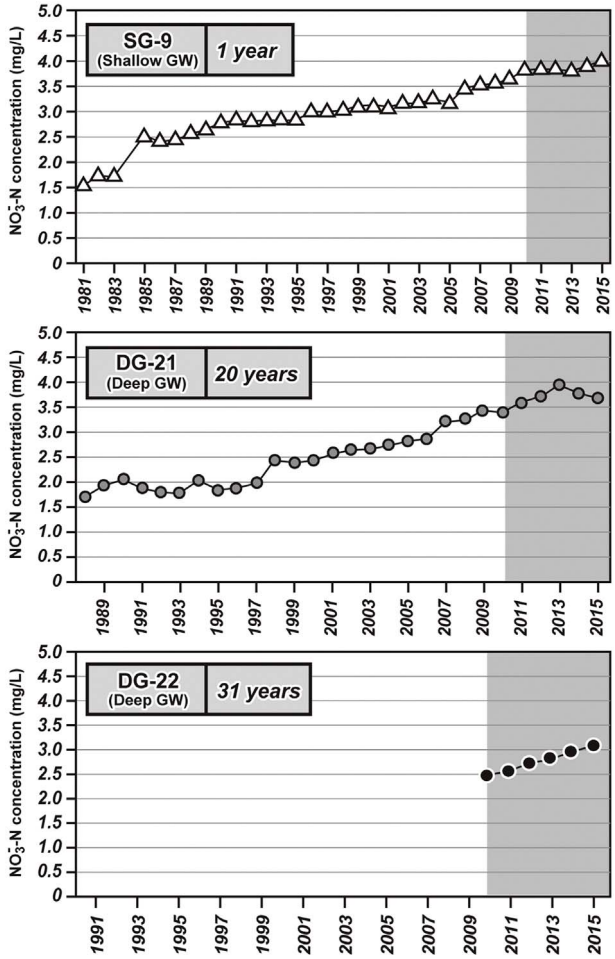

Fig. 10. Long-term fluctuation of NO_3^-–N concentration at three locations in Area C (the shaded area corresponds to Fig. 10).

shallow groundwater sample (SG-9, ^{85}Kr apparent age: 1year) displays an increasing tendency with seasonal fluctuations: a fall in the summer season and a rise in the winter season. These fluctuations imply an effect of dilution by abundant recharge water derived from precipitation during summer, which may reflect the infiltration of young water to this location.

Deep groundwater collected from DG-22 yielded an apparent age of 31 years. The NO_3^- concentration of that well displayed a linear increasing trend without clear fluctuations; thus, this groundwater is flowing after having been well mixed. On the other hand,

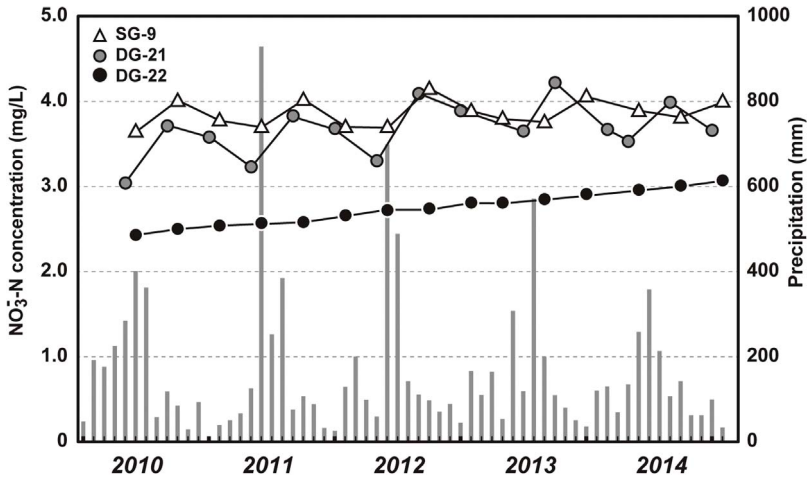

Fig. 11. Monthly fluctuation of NO_3^-–N concentration in three locations in Area C between 2010 and 2014.

the deep groundwater at DG-21 will be seasonally affected by the contribution of young groundwater provided by irrigation of paddy fields in the summer season. This finding is supported by the changes in groundwater level (Fig. 2) and fluctuations in NO_3^-–N concentration at this well, resulting in the age of this well being younger (20 years) compared to DG-22.

Although an apparent groundwater age of DG-21 is older than SG-9, the nitrate levels and its fluctuation patterns are similar for the two wells. To obtain a better understanding of groundwater age, the temporal variation of nitrate input are needed. Since the nitrate input information was insufficient in this study, further study focusing on the nitrate concentration and groundwater age as reported in the previous studies (Gourcy et al., 2009; Koh et al., 2006) is needed.

5. Conclusions

Groundwater age could not be estimated using the analytical results for CFCs or SF_6. The reason for this was regarded as artificial additions to the concentration in almost the entire study area; the trend was more pronounced in urban areas and industrial areas. However, even in these regional circumstances, the apparent groundwater ages of approximately 16 years, 36 years, and not less than 55 years were obtained from ^{85}Kr measurements in the recharge area, the discharge area, and the stagnant zone of groundwater, respectively, along the A–A' line. These results matched the local groundwater flow system in which the age increased from the recharge area to the discharge area. This trend was also supported by the lumped parameter model analysis using with ^3H. In contrast, along the B–B' line, the age of not less than 55 years and the lack of detected CFCs and SF_6 imply old (stagnant-type) groundwater: this tendency corresponds to the occurrence of denitrification. In Area C, which is considered to be a high-nitrate-input area, very young apparent ages for the shallow groundwater and around 20–30 years for the deep groundwater were estimated. These values are reasonable when compared to the long-term fluctuations of the NO_3^-–N concentration. Accordingly, there is the possibility that the current nitrate input will appear in deep groundwater in a few decades.

In the Kumamoto area groundwater accounts for almost 100% of the drinking water resources, but emergent concerns have included contamination by nitrate nitrogen. It is hoped that the specific age of groundwater can be used effectively as a "time axis" for sustainable groundwater conservation and healthy management/conservation in this area.

Acknowledgment

We thank Mr. Reo Ikawa and Mr. Masahiko Ono of AIST, the Geological Survey of Japan for their help during field surveys. We also thank Mr. Tomohisa Ishii and Ms. Risako Soezima for a fruitful discussion. A part of this study was funded by a CREST Project (JST: Japan Science and Technology Agency) with additional support from the Grant-in-Aid for Young Scientists (B) (no. 26870448).

References

Alikhani, J., Deinhart, A.L., Visser, A., Bibby, R.K., Purtschert, R., Moran, J.E., 2016. Nitrate vulnerability projections from Bayesian inference of multiple groundwater age tracers. J. Hydrol. 543, 167–181.

Aoyama, M., Fujii, K., Hirose, K., Igarashi, Y., Isogai, K., Nitta, W., Sartorius, H., Schlosser, C., Weiss, W., 2008. Establishment of a cold charcoal trap-gas chromatography-gas counting system for ^{85}Kr measurements in Japan and results from 1995 to 2006. Technical Reports of the Meteorological Research Institute, vol. 54.

Asai, K., Tsujimura, M., 2009. Dating method for young groundwater using environmental tracers −Application of CFCs dating method to spring in volcanic areas. J. Jpn. Assoc. Hydrol. Sci. 39, 67–78. http://dx.doi.org/10.4145/jahs.39.67. (in Japanese).

Asai, K., Tsujimura, M., Fantong, W.Y., Satake, H., 2011. Impact of natural and local anthropogenic SF6 sources on dating springs and groundwater using SF_6 in central Japan. Hydrol. Res. Lett. 5, 42–46.

Böhlke, J.K., 2006. TRACERMODEL1. Excel workbook for calculation and presentation of environmental tracer data for simple groundwater mixtures. In: IAEA (Ed.), Use of Chlorofluorocarbons in Hydrology. IAEA, Vienna, pp. 239–243.

Begemann, F., Libby, W.F., 1957. Continental water balance, groundwater inventory and storage times, surface ocean mixing rates and world-wide water circulation patterns from cosmic ray and bomb tritium. Geochim. Cosmochim. Acta 12, 277–296.

Busenberg, E., Plummer, L.N., 1992. Use of chlorofluorocarbons (CCl3F and CCl2F2) as hydrologic tracers and age-dating tools: the alluvium and terrace system of central Oklahoma. Water Resour. Res. 28, 2257–2283.

Busenberg, E., Plummer, L.N., 2000. Dating young ground water with sulfur hexafluoride–Natural and anthropogenic sources of sulfur hexafluoride. Water Resour. Res. 36, 3011–3030.

Cauwels, P., Buysse, J., Poffijn, A., Eggermont, G., 2001. Study of the atmospheric ^{85}Kr concentration growth in Gent between 1979 and 1999. Radiat. Phys. Chem. 61, 649–651.

Cook, P.G., Solomon, D.K., 1997. Recent advances in dating young groundwater: chlorofluorocarbons, H-3/He-3 and Kr-85. J. Hydrol. 191, 245–265.

Egboka, B.C.E., Cherry, J.A., Farrolden, R.N., Frind, E.O., 1983. Migration of contaminants in groundwater at a landfill: a case study, 3. Tritium as an indicator of dispersion and recharge. In: In: Cherry, J.A. (Ed.), Migration of Contaminants in Groundwater at a Landfill: A Case Study, vol. 63. pp. 51–80 Journal of Hydrology.

Gal, C.L., Salle, L., Aquilina, L., Fourre, E., Jean-baptiste, P., Michelot, J., Roux, C., Bugai, D., Labasque, T., 2012. Groundwater residence time downgradient of Trench No. 22 at the Chernobyl Pilot Site: constraints on hydrogeological aquifer functioning. Appl. Geochem. 27 (7), 1304–1319. http://dx.doi.org/10.1016/j.apgeochem.2011.12.006.

Gooddy, D.C., Darling, W.G., Abesser, C., Lapworth, D.J., 2006. Using chlorofluorocarbons (CFCs) and sulphur hexafluoride (SF_6) to characterise groundwater movement and residence time in a lowland Chalk catchment. J. Hydrol. 330, 44–52. http://dx.doi.org/10.1016/j.jhydrol.2006.04.011.

Gourcy, L., Baran, N., Vittecoq, B., 2009. Improving the knowledge of pesticide and nitrate transfer processes using age-dating tools (CFC, SF_6, ^3H) in a volcanic island (Martinique French West Indies). J. Contam. Hydrol. 108 (3), 107–117.

Green, M.B., Wollheim, W.M., Basu, N.B., Gettel, G., Rao, P.S., Morse, N., Stewart, R., 2009. Effective denitrification scales predictably with water residence time across diverse systems. Nat. Proc. Available at: http://precedings.nature.com/documents/3520/version/1, (Date accessed: 26 May 2017).

Hanshaw, B.B., Back, W., Rubin, M., 1965. Radiocarbon determinations for estimating groundwater flow velocities in Central Florida. Science 148, 494–495.

Heilweil, V.M., Solomon, D.K., Gingerich, S.B., Verstraeten, I.M., 2009. Oxygen, hydrogen, and helium isotopes for investigating groundwater systems of the Cape Verde Islands, West Africa. Hydrol. J. 17, 1157–1174.

Hosono, T., Tokunaga, T., Kagabu, M., Nakata, H., Orishikida, T., Lin, I.T., 2013. The use of $\delta^{15}N$ and $\delta^{18}O$ tracers with an understanding of groundwater flow dynamics for evaluating the origins and attenuation mechanisms of nitrate pollution. Water Res. 47, 2661–2675.

IAEA, 2006. Use of Chlorofluorocarbons in Hydrology: A Guidebook. International Atomic Energy Agency, Vienna 277p.
Ichikawa, T., 2004. The recent drawdown of groundwater discharge at Kumamoto area and the importance of the mid-stream area of River Shira. Proceedings of Symposium on Healthy Groundwater Cycle from the Aspect of Quality and Quantity Sponsored by the Japanese Association of Groundwater Hydrology 21–28.
Johnston, C.T., Cook, P.G., Frape, S.K., Plummer, L.N., Busenberg, E., Blackport, R.J., 1998. Ground water age and nitrate distribution within a glacial aquifer beneath a thick unsaturated zone. Ground Water 36, 171–180.
Kagabu, M., Shimada, J., Shimano, Y., Higuchi, S., Noda, S., 2011. Groundwater flow system in Aso caldera. J. Jpn. Assoc. Hydrol. Sci. 41, 1–17 (in Japanese).
Kayane, I., Yasuo, S., Tanaka, N., 1987. Groundwater flow system around the south western foot of Aso volcano. J. Jpn. Assoc. Hydrol. Sci. 17, 111–120 (in Japanese).
Kayane, I., 1980. Hydrology. Daimeido, Tokyo 272 (in Japanese).
Kazahaya, K., Yasuhara, M., 1994. A hydrogen isotopic study of spring in Mt. Yatsugatake, Japan: application to groundwater recharge and flow processes. J. Jpn. Assoc. Hydrol. Sci. 24, 107–119 (in Japanese).
Kazahaya, K., Yasuhara, M., Takahashi, H., Morikawa, N., Ohwada, M., Tosaki, Y., Asai, K., 2007. Groundwater studies using isotopes and noble gases as a tracer: review and prospect. J. Jpn. Assoc. Hydrol. Sci. 37, 221–252 (in Japanese).
Kimura, S., 1986. Behavior analysis of subsurface water using contained radioisotopes. Bull. Natl. Res. Inst. Agric. Eng. 25, 1–91 (in Japanese).
Koh, D.C., Plummer, L.N., Solomon, D.K., Busenberg, E., Kim, Y., Chang, H.-W., 2006. Application of environmental tracers to mixing, evolution, and nitrate contamination of ground water in Jeju Island, Korea. J. Hydrol. 327, 258–275.
Koh, D.C., Plummer, N., Busenberg, E., Kim, Y., 2007. Evidence for terrigenic SF_6 in groundwater from basaltic aquifers, Jeju Island, Korea: implications for groundwater dating. J. Hydrol. 339, 93–104.
Kosaka, H., Shimada, J., Sakamoto, M., 2002. The origin of the groundwater in the Kumamoto area by using a stable isotope ratio. Proceedings of Annual Meeting of Japanese Association of Groundwater Hydrology 140–143.
Kralik, M., Humer, F., Fank, J., Harum, T., Klammler, G., Gooddy, D., Sültenfuß, J., Gerber, C., Purtschert, R., 2014. Using $^{18}O/^{2}H$, $^{3}H/^{3}He$, ^{85}Kr and CFCs to determine mean residence times and water origin in the Grazer and Leibnitzer Feld groundwater bodies (Austria). Appl. Geochem. 50, 150–163.
Kumamoto prefecture and Kumamoto city, 1995. The Investigation Report on the Groundwater Protection and Management in Kumamoto Area, Kumamoto, Japan. 122 (in Japanese).
Loosli, H.H., Lehmann, B.E., Smethie, W.M., 2000. Noble gas radioisotopes: ^{37}Ar, ^{85}Kr, ^{39}Ar, ^{81}Kr. In: Cook, P.G., Herezeg, A.L. (Eds.), Environmental Tracers in Subsurface Hydrology. Kluwer Academic Publishers, Boston, pp. 379–396.
Loosli, H.H., 1992. Applications of ^{37}Ar, ^{39}Ar and ^{85}Kr in hydrology, oceanography, and atmospheric studies: current state of the art. In: isotopes of Noble Gases as Tracers in Environmental Studies. In: Proceedings of a Consultants Meeting, International Atomic Energy Agency. Vienna. pp. 73–85.
Mahara, Y., 1995. Noble gases dissolved in groundwater in a volcanic aquifer: helium Isotopes in the Kumamoto Plain. Environ. Geol. 25, 215–224.
Maloszewski, P., Zuber, A., 1982. Determining the turnover time of groundwater systems with the aid of environmental tracers 1. Models and their applicability. J. Hydrol. 57, 207–231.
Momoshima, N., Inoue, F., Sugihara, S., Shimada, J., Taniguchi, M., 2010. An improved method for ^{85}Kr analysis by liquid scintillation counting and its application to atmospheric ^{85}Kr determination. J. Environ. Radioact. 101, 615–621.
Momoshima, N., Inoue, F., Ohta, T., Mahara, Y., Shimada, J., Ikawa, R., Kagabu, M., Ono, M., Yamaguchi, K., Sugihara, S., Taniguchi, M., 2011. Application of ^{85}Kr dating to groundwater in volcanic aquifer of Kumamoto Area, Japan. J. Nucl. Chem. 287, 761–767. http://dx.doi.org/10.1007/s10967-010-0821-0.
Nir, A., 1964. On the interpretation of tritium age measurements in groundwater. J. Geophys. Res. 69, 2589–2595.
Ocampo, C.J., Oldham, C.E., Sivapalan, M., 2006. Nitrate attenuation in agricultural catchments: sifting balances between transport and reaction. Water Resour. Res. 42, W01408. http://dx.doi.org/10.1029/2004WR003773.
Ohta, T., Mahara, Y., Momoshima, N., Inoue, F., Shimada, J., Ikawa, R., Taniguchi, M., 2009. Separation of dissolved Kr from a water sample by means of a hollow fiber membrane. J. Hydrol. 376, 152–158.
Okai, T., Takashima, Y., Shiraishi, N., Matsuoka, N., 1984. Measurement of Krypton-85 in the atmosphere with a portable apparatus. J. Radioanal. Nucl. Chem. 81, 161–165.
Ozyurt, N.N., Bayari, C.S., 2003. LUMPED: a Visual Basic code of lumped-parameter models for mean residence time analyses of groundwater systems. Comput. Geosci. 29, 79–90.
Pearson, F.J., White, D.E., 1967. Carbon 14 ages and flow rates of water in carrizo sand, atascosa county, texas. Water Resour. Res. 3, 251–261.
Plummer, L.N., Busenberg, E., Drenkard, S., Schlosser, P., McConnell, J.B., Michel, R.L., Ekwurzel, B., Weppernig, R., McConnell, J.B., Michel, R.L., 1998. Flow of river water into a karstic limestone aquifer-2 Dating the young fraction in groundwater mixtures in the Upper Floridan aquifer near Valdosta, Georgia. Appl. Geochem. 13, 1017–1043.
Schroder, K.J.P., Roether, W., 1975. The releases of krypton-85 and tritium to the environment and tritium to krypton-85 ratios as source indicators. Isotope Ratios as Pollutant Source and Behaviour Indicators. International Atomic Energy Agency, Vienna, pp. 231–253.
Seelmann-Eggebert, W., Pfennig, G., Munzel, H., Klewe-Nebenius, H., 1981. Nuklidkarte. Kernforschungszentrum Karlsruhe, Karlsruhe, pp. 32.
Seitzinger, S., Harrison, J.A., Böhlke, J.K., Bouwman, A.F., Lowrance, R., Peterson, B., Tobias, C., Drecht, G.V., 2006. Denitrification across landscapes and waterscapes: a synthesis. Ecol. Appl. 16 (6), 2064–2090.
Shevenell, L., Goff, F., 1995. The use of tritium in groundwaters to determine fluid mean residence times of Valles Caldera hydrothermal fluids, New Mexico, U.S.A. J. Volcanol. Geotherm. Res. 67, 187–205.
Shimada, J., Ichiyanagi, K., Kagabu, M., Saita, S., Mori, K., 2012. Effect of artificial recharge using abandoned rice paddies for the sustainable groundwater management in Kumamoto, Japan. Proceedings of World Environmental and Water Resources Congress 2012, 59–69.
Simpson, B., Carmi, I., 1983. The hydrology of the Jordan tributaries (Israel): hydrographic and isotopic investigation. J. Hydrol. 62, 225–242.
Stockburger, H., Sartorius, H., Sittkus, A., 1977. Method for measurement of kr-85 and xenon-113-content in atmosphere. Z Naturforschung A32, 1249–1253.
Stuart, M.E., Maurice, L., Heaton, T.H.E., Sapiano, M., Sultana, M.M., Gooddy, D.C., Chilton, P.J., 2010. Applied Geochemistry Groundwater residence time and movement in the Maltese islands–A geochemical approach. Appl. Geochem. 25 (5), 609–620. http://dx.doi.org/10.1016/j.apgeochem.2009.12.010.
Sturchio, N.C., Du, X., Purtschert, R., Lehmann, B.E., Sultan, M., Patterson, L.J., Lu, Z.T., Müller, P., Bigler, T., Bailey, K., O'Connor, T.P., Young, L., Lorenzo, R., Becker, R., El Alfy, Z., El Kaliouby, B., Dawood, Y., Abdallah, A.M.A., 2004. One million year old groundwater in the Sahara revealed by krypton-81 and chlorine-36. Geophys. Res. Lett. 31.
Tomášek, M., Wilhelmova, L., 1997. Development of ^{85}Kr atmospheric activity and comparison with prognosis. J. Radioanal. Nucl. Chem. 218, 119–121.
USGS, 2016. Air Curve in The Reston Chlorofluorocarbon Laboratory. http://water.usgs.gov/lab/software/air_curve/index.html, (Accessed 21 July 2016).
Visser, A., Bibby, R., Moran, J., Singleton, M., Esser, B., 2015. California GAMA special study: development of a capability for the analysis of Krypton-85 in groundwater samples. Final Report for the California State Water Resources Control Board. (25p).
Vuataz, F.D., Goff, F., 1986. Isotope geochemistry of thermal and nonthermal waters in the Valles caldera, Jemez Mountains, northern New Mexico. J. Geophys. Res. 91, 1835–1853.
Wilhelmová, L., Tomášek, M., Stukheil, K., 1990. Kr-85 activity in the atmosphere of Prague from 1983 to 1988. J. Radioanal. Nucl. Chem. 144, 125–134.
Winger, K., Feichter, J., Kalinowski, M.B., Sartorius, H., Schlosser, C., 2005. A new compilation of the atmospheric ^{85}krypton inventories from 1945 to 2000 and its evaluation in a global transport model. J. Environ. Radioact. 80, 183–215.
Yabusaki, S., Tsujimura, M., Tase, N., 2003. Recent Trend of Tritium Concentration in Precipitation in Kanto Plane, Japan, vol. 4. Bulletin of the Terrestrial Environment Research Center the University of Tsukubapp. 119–124 (in Japanese).
Yoshino, M., 1986. Chimate in a Small Area. Chijin Shokan, Tokyo 320p (in Japanese).